Supporting Information for

SERS-based molecularly imprinted plasmonic sensor for highly sensitive PAH detection

Alexander Castro Grijalba,[a,b,†] Verónica Montes-García,[a,†] María José Cordero-Ferradás,[a] Eduardo Coronado,[b] Jorge Pérez-Juste[a,*] and Isabel Pastoriza-Santos[a,*]

[a] *Centro Singular de Investigaciones biomédicas (CINBIO) y Departamento de Química Física, Universidade de Vigo, 36310 Vigo, Spain*

[b] *INFIQC, Centro Láser de Ciencias Moleculares, Departamento de Fisicoquímica, Facultad de Ciencias Químicas, Universidad Nacional de Córdoba, Córdoba 5000, Córdoba, Argentina.*

† These authors have contributed equally to the work

Corresponding Authors

*E-mail: pastoriza@uvigo.es (I.P.-S.).

*E-mail: juste@uvigo.es (J.P.-J.).

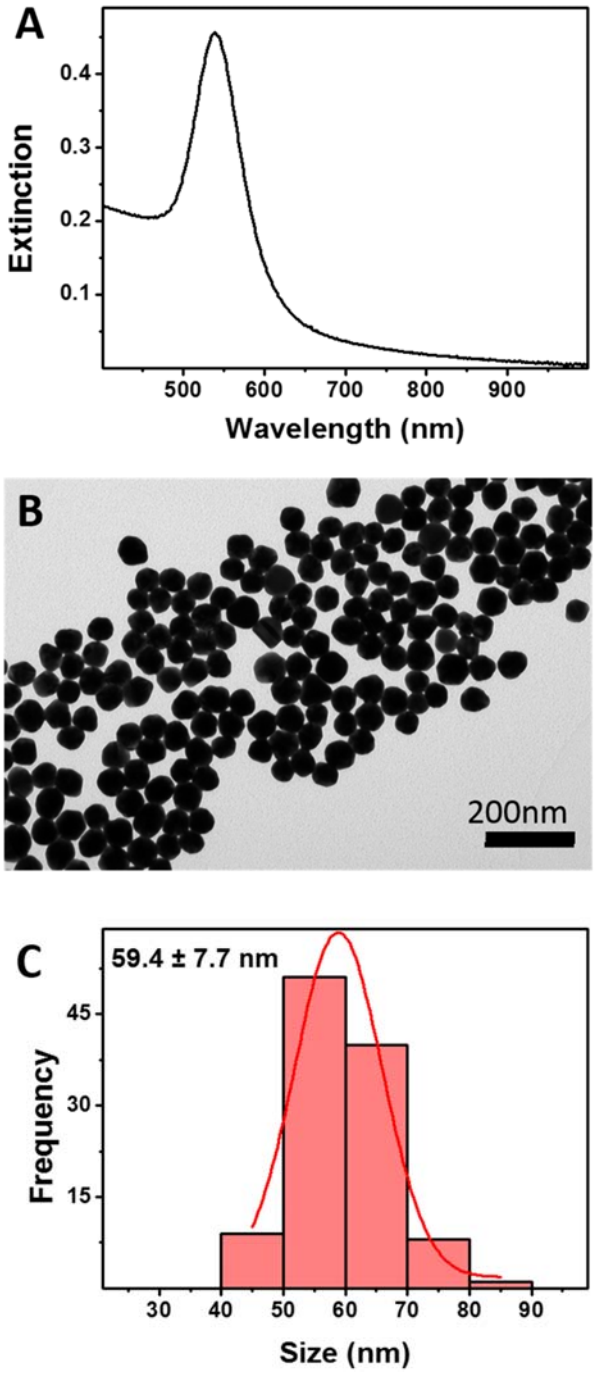

Figure S1. (A) Vis-NIR extinction spectrum of citrate-stabilized Au nanoparticles in water. (B) Representative TEM image. (C) Size distribution histogram obtained from TEM analysis.

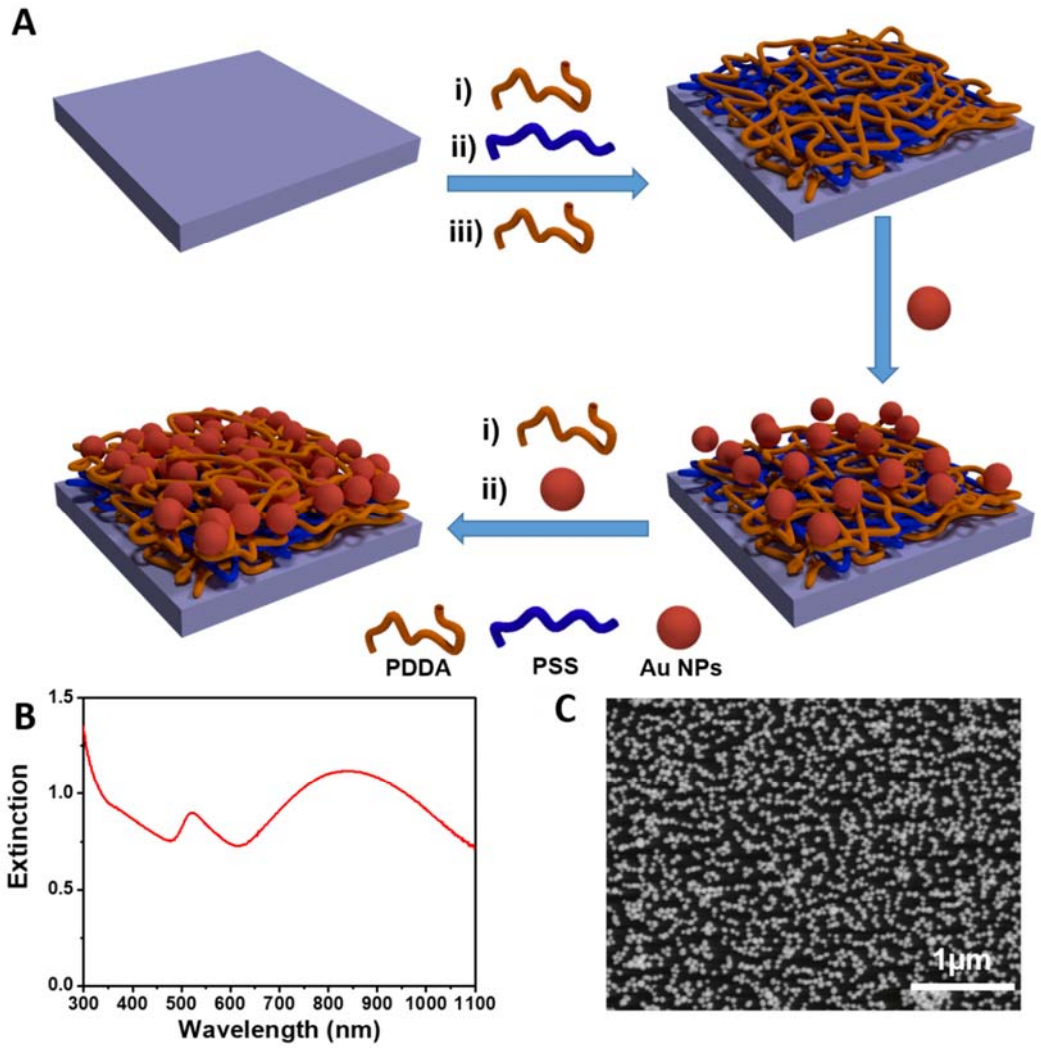

Figure S2. (A) Schematic representation of Au NPs assemblies fabricated by Layer-by-Layer deposition, (B) UV-Vis−NIR extinction spectra and (C) SEM images of Au NPs assemblies on positively charged PDDA modified glass obtained after two depositions cycles.

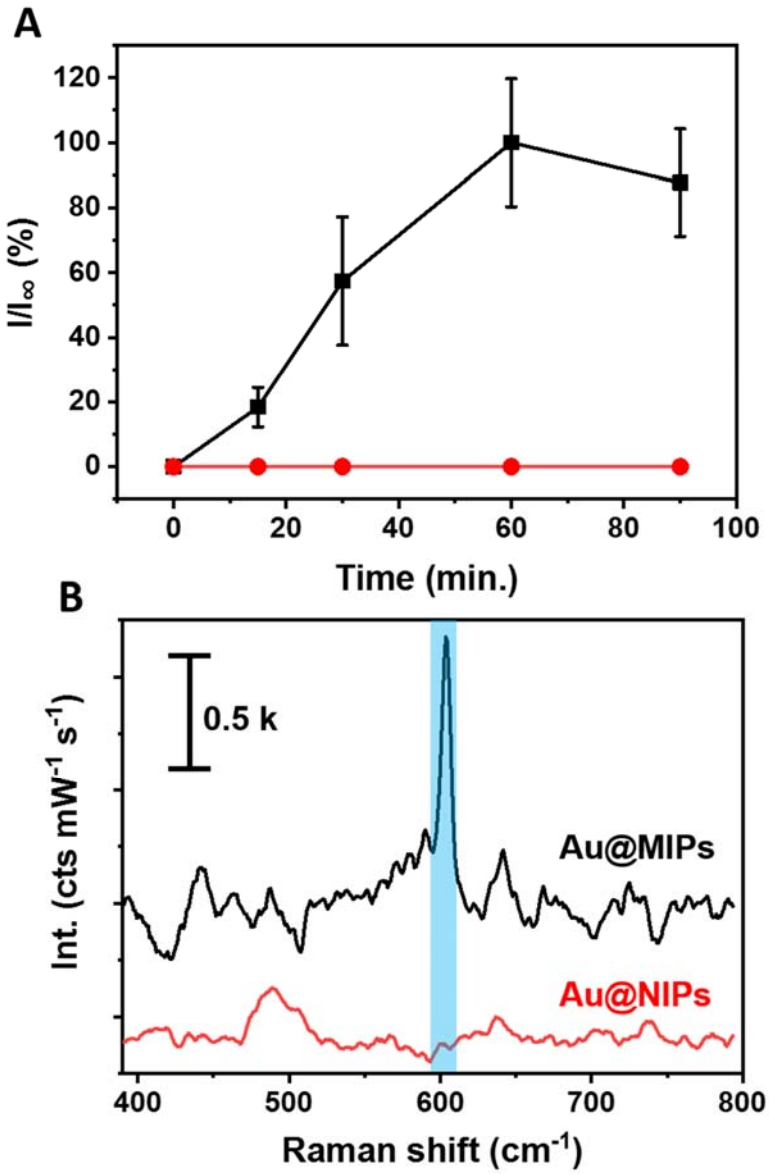

Figure S3. (A) Time-dependent normalized SERS intensity at 594 cm^{-1} upon the uptake of 10^{-8} M pyrene by pyrene-based Au@MIPs (black) and Au@NIPs (red). (B) Representative SERS spectra after 60 min of incubation of pyrene-based Au@MIPs (black) and Au@NIPs (red) in an aqueous solution containing 10^{-8} M pyrene. I_∞ is the SERS intensity at 594 cm^{-1} for Au@MIPs when saturation is reached.

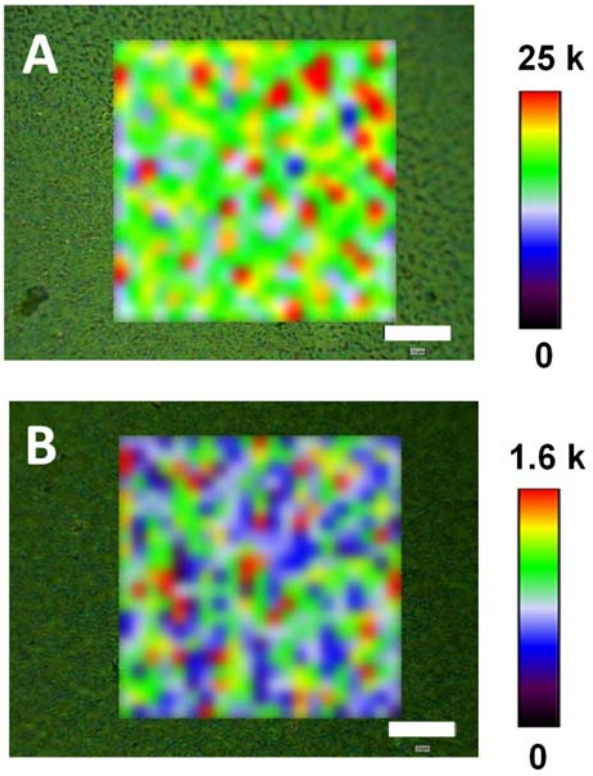

Figura S4. SERS mapping analysis at 594 cm^{-1} of pyrene at 10^{-5} M (top) and 10^{-9} M (bottom). SERS measurements were performed using pyrene-based Au@MIPs with a 785 nm laser line, a 50× objective, 0.5 s acquisition time and 1.74 mW maximum power.

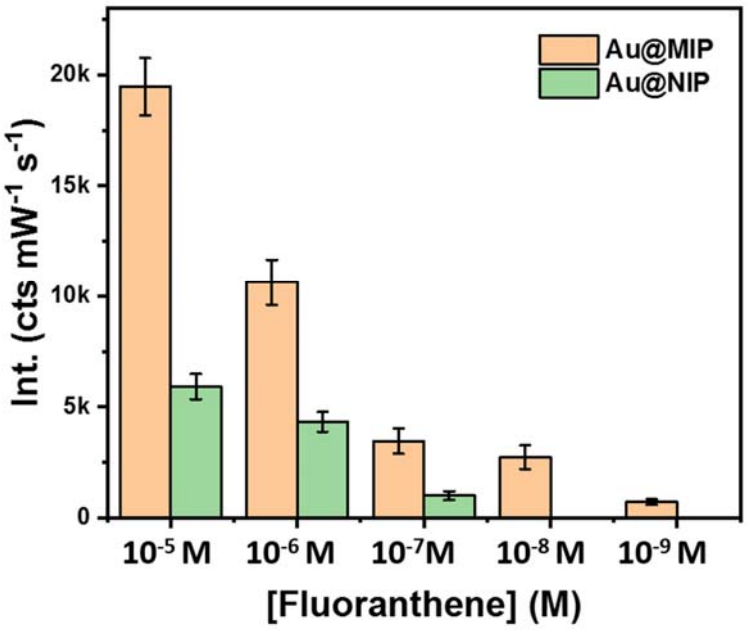

Figure S5. Averaged SERS Intensity at 557 cm^{-1} as a function of fluoranthene concentration for fluoranthene-based Au@MIP and Au@NIP substrates. SERS measurements were performed with a 785 nm laser line, a 50× objective, 0.5 s acquisition time and 1.74 mW maximum power. For fluoranthene concentrations ranging from 10^{-5} to 10^{-8} M, averaged calculation was performed with 20 points. For 10^{-9} M fluoranthene concentration, averaged calculation was performed with 441 points.

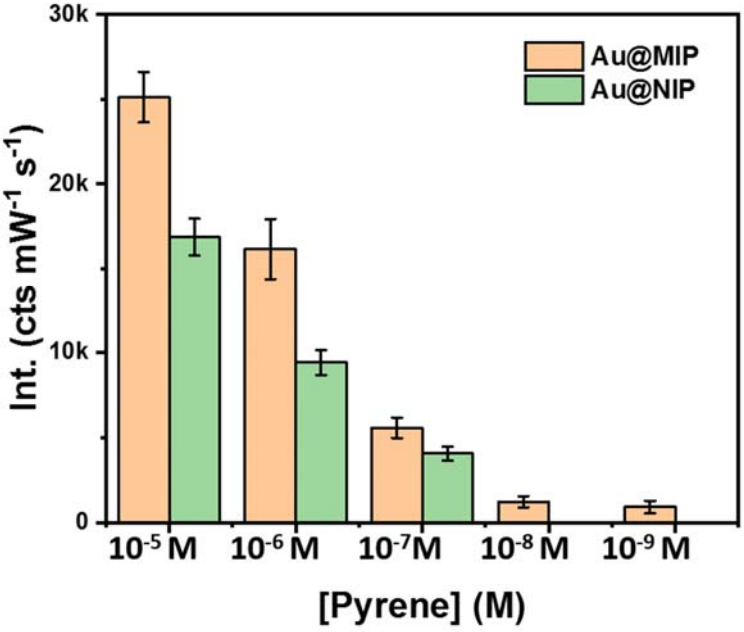

Figure S6. Averaged SERS Intensity at 594 cm^{-1} as a function of pyrene concentration obtained for Au@MIP and Au@NIP substrates. SERS measurements were performed with a 785 nm laser line, a 50× objective, 0.5 s acquisition time and 1.74 mW maximum power. For pyrene concentrations ranging from 10^{-5} to 10^{-8} M, the intensity corresponds to the average of 20 measurements. For 10^{-9} M pyrene concentration, averaged intensity was calculated with 441 points.

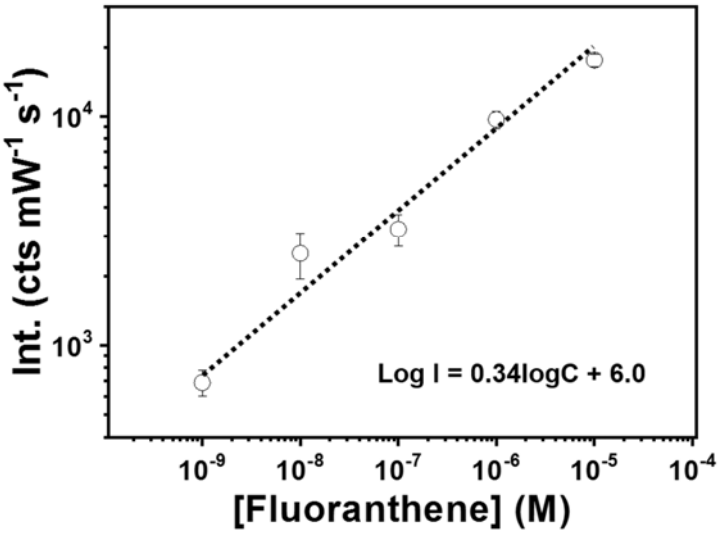

Figure S7. SERS intensity at 665 cm^{-1} as a function of fluoranthene concentration. SERS measurements were performed with a 785 nm laser line, a 50× objective, 0.5 s acquisition time and 1.74 mW maximum power.

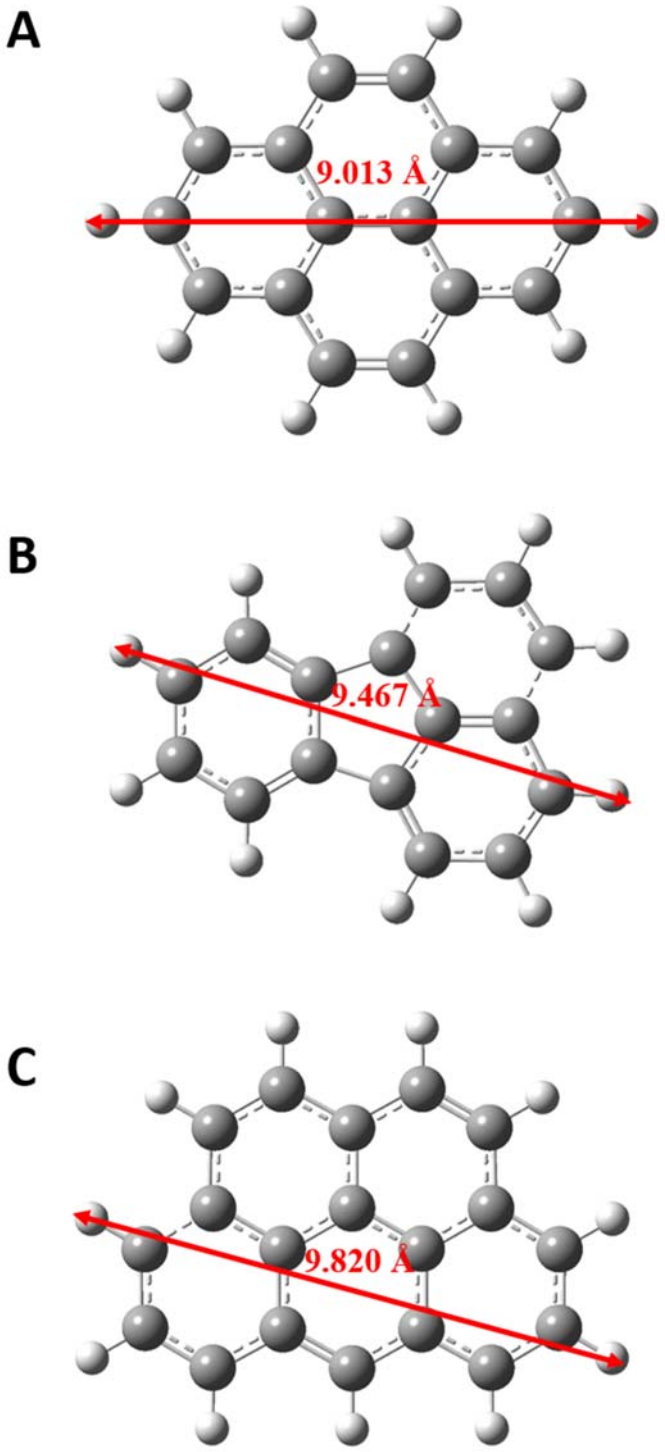

Figure S8. Optimized geometries of: (A) pyrene, (B) fluoranthene and (C) benzo[a]pyrene. In each case the maximum length between atoms is highlighted in red.

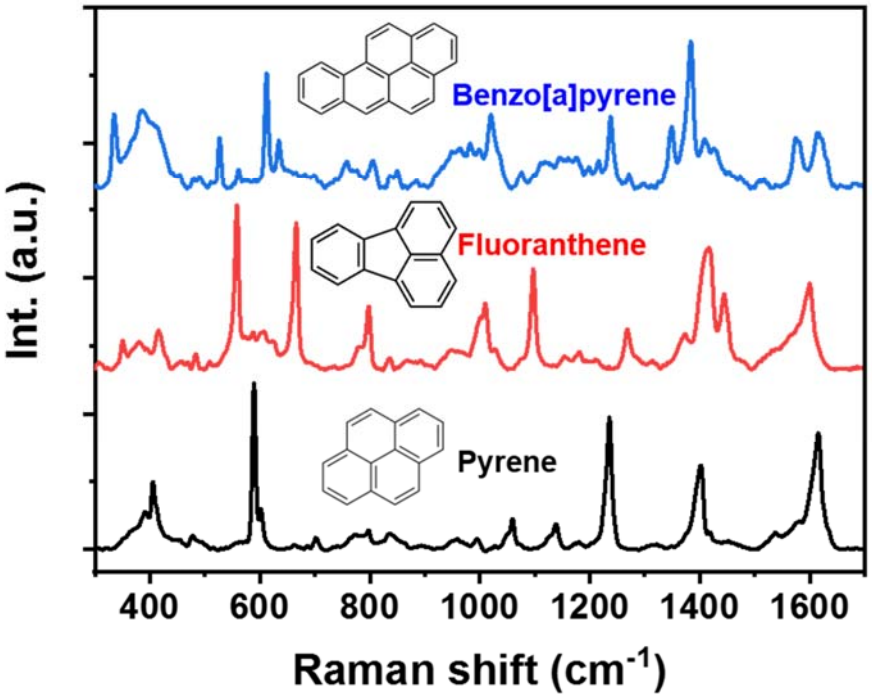

Figure S9. Representative long-range SERS spectra of benzo[a]pyrene (blue), fluoranthene (red) and pyrene (black).

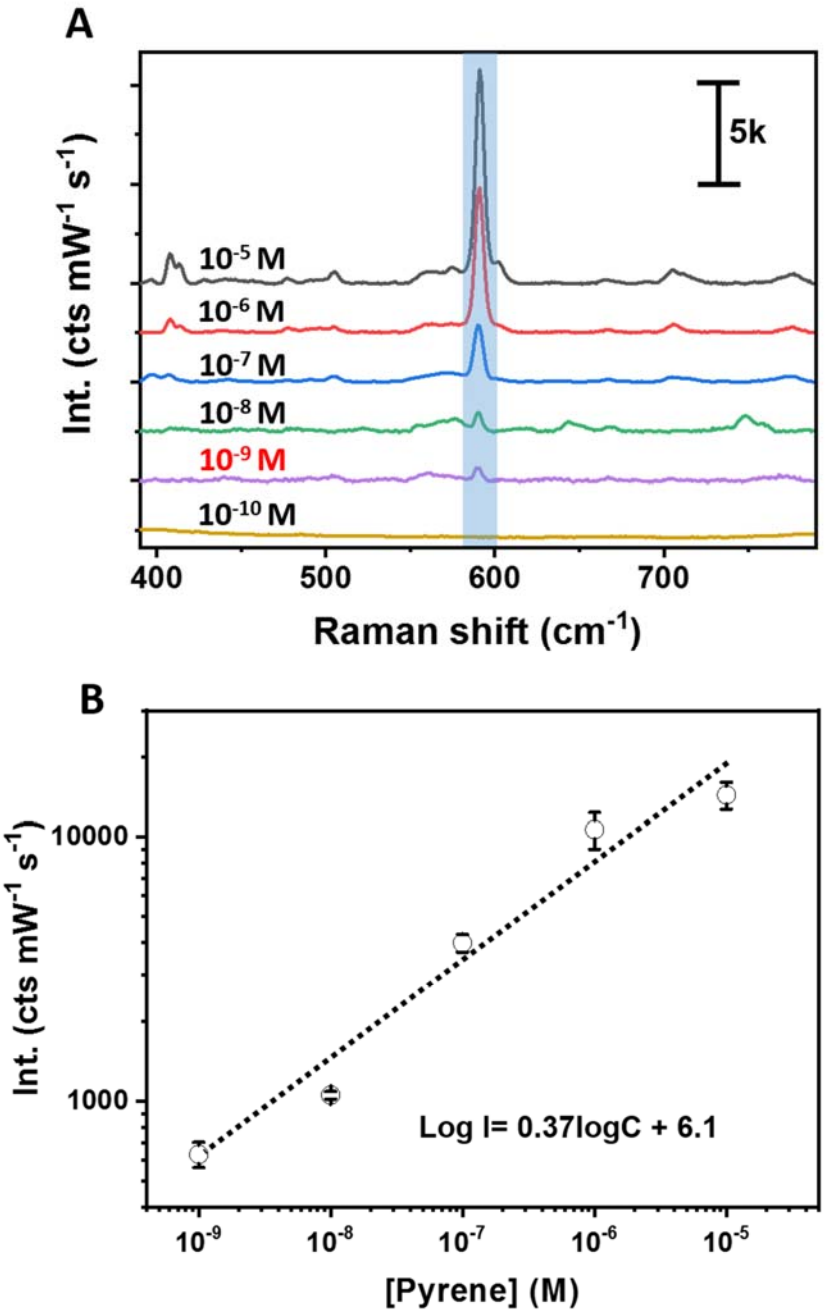

Figure S10. (A) SERS spectra of pyrene obtained from spiked seawater solutions at different concentrations. (B) SERS intensity at 594 cm^{-1} as a function of pyrene concentration

Table S1. Summary of the vibrational band assignments for pyrene, fluoranthene and benzo[a]pyrene.

Pyrene 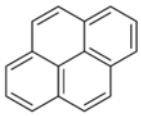		**Flouranthene** 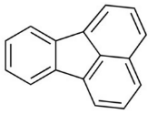		**Benzo[a]pyrene** 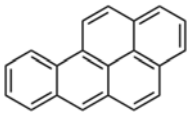	
Raman shift / cm^{-1}	**Assignment**	**Raman shift / cm^{-1}**	**Assignment**	**Raman shift / cm^{-1}**	**Assignment**
1614	C-C stretching[1]	**1605**	C-C stretching[2]	**1618**	C-C stretching[2]
1401	C-C stretching[1]	**1450**	C-C stretching[2]	**1576**	C-C stretching[2]
1235	C-C stretching[1]	**1414**	C-C stretching[2]	**1421**	C-C stretching[2]
1139	C-H in plane bending[1]	**1406**	Ring vibration[2]	**1404**	C-C stretching[2]
1060	C-H in plane bending[1]	**1262**	C-H-in-plane bending[2]	**1383**	C-C stretching[2]
590	Ring breathing[1]	**1097**	C-H-in-plane bending[2]	**1233**	C-H-in-plane bending[2]
407	Ring deformation[1]	**1013**	C-C stretching[2]	**1207**	C-H-in-plane bending[2]
		795	C-H stretching[2]	**1015**	C-H-in-plane bending[2]
		665	C-H stretching[2]	**632**	C-H stretching[2]
		553	Skeletal stretching[2]	**605**	C-H stretching[2]
		470	Skeletal stretching[2]	**513**	Skeletal stretching[2]
				327	Skeletal deformation[2]

References

(1) Montes-García, V.; Fernández-López, C.; Gómez, B.; Pérez-Juste, I.; García-Río, L.; Liz-Marzán, L. M.; Pérez-Juste, J.; Pastoriza-Santos, I. Pillar[5]arene-Mediated Synthesis of Gold Nanoparticles: Size Control and Sensing Capabilities. *Chemistry – A European Journal* **2014**, *20*, 8404-8409.

(2) Qu, L.-L.; Li, Y.-T.; Li, D.-W.; Xue, J.-Q.; Fossey, J. S.; Long, Y.-T. Humic acids-based one-step fabrication of SERS substrates for detection of polycyclic aromatic hydrocarbons. *Analyst* **2013**, *138*, 1523-1528.